Supporting information for

Switching of the redox centers of a tris-2-mercaptophenolato chromium(III) metalloligand by a guest metal ion

Masanori Wakizaka,[a,b]* Takeshi Matsumoto,[a] and Ho-Chol Chang[a,]*

[a] Department of Applied Chemistry, Faculty of Science and Engineering, Chuo University,

1-13-27 Kasuga, Bunkyo-ku, Tokyo 112-8551, Japan

[b] Frontier Research Institute for Interdisciplinary Sciences, Tohoku University,

6-3 Aramaki-Aza-Aoba, Aoba-ku, Sendai 980-8578, Japan.

E-mail: masanori.wakizaka.a7@tohoku.ac.jp (M. W.) and chang@kc.chuo-u.ac.jp (H.-C. C.)

Contents

Methods

Materials. $CoCl_2 \cdot 6H_2O$, $Co(ClO_4)_2 \cdot 6H_2O$, KOH, and tetra-*n*-butylammonium hexafluorophosphate ($[n\mathrm{Bu}_4\mathrm{N}]PF_6$) were purchased from Wako Pure Chemical Industries (Japan). Dehydrated MeOH and dehydrated MeCN were purchased from Kanto Chemical Co. Inc (Japan). Tetramethylammonium hydroxide pentahydrate ($[\mathrm{Me}_4\mathrm{N}]OH \cdot 5H_2O$) and 2-mercaptophenol ($mpH_2$) were purchased from Tokyo Kasei Kogyo Co. Ltd (Japan). All solvents used were degassed by N_2 bubbling and following five freeze-pump-thaw cycles immediately prior to use. $[\mathrm{Me}_4\mathrm{N}]_3[\textit{fac}\text{-}\mathrm{Cr}^{\mathrm{III}}(\mathrm{mp})_3]$ and $[K_3\{\textit{fac}\text{-}\mathrm{Cr}^{\mathrm{III}}(\mathrm{mp})_3\}(H_2O)_6]_n$ were prepared according the reported procedures.[33] **Caution!** Although we did not experience any difficulties with perchlorate salts, these should be regarded as potentially explosive, and therefore handled with the utmost care.

$K_y[\mathrm{Co}^{\mathrm{II}}(H_2O)_6]_{1.5-0.5y}[\mathrm{Co}^{\mathrm{III}}\{\textit{fac}\text{-}\mathrm{Cr}^{\mathrm{III}}(\mathrm{mp})_3\}_2] \cdot xH_2O$ ($\mathbf{1} \cdot xH_2O$). Adding a pink aqueous solution (10 mL) of $CoCl_2 \cdot 6H_2O$ (95.0 mg, 0.399 mmol) to a green aqueous solution (10 mL) of $[K_3\{\textit{fac}\text{-}\mathrm{Cr}^{\mathrm{III}}(\mathrm{mp})_3\}(H_2O)_6]_n$ (200 mg, 0.299 mmol) afforded an olive-green suspension after stirring for 1 h under an atmosphere of N_2 using Schlenk-line techniques. After filtration, an olive-green solution was obtained, whose color turned to purple upon exposure to air. From this solution, purple crystals were obtained after standing for 1 day. After filtration and washing with water (3 × 5 mL), followed by drying *in vacuo*, complex $\mathbf{1} \cdot xH_2O$ was isolated in the form of violet crystals in 15% yield. The crystals of $\mathbf{1} \cdot xH_2O$ easily loss the crystal and hydrated water molecules under drying *in vacuo*. Anal. Found: C, 38.20; H, 3.38%. Calc. for $C_{36}H_{39.6}Co_{2.4}Cr_2K_{0.2}O_{13.8}S_6$ ($\mathbf{1}$–$0.6H_2O$, y = 0.2): C, 37.97; H, 3.51%. ICP-AES Found: Co, 12.4; Cr, 9.43; K, 0.77%. Calc. for $\mathbf{1}$–$0.6H_2O$ (y = 0.2): Co, 12.4; Cr, 9.13, K, 0.69%. Violet

single crystals suitable for X-ray diffraction analysis were obtained by layering an aqueous solution of $CoCl_2 \cdot 6H_2O$ onto an aqueous solution of $[K_3\{fac\text{-}Cr^{III}(mp)_3\}(H_2O)_6]_n$.

Physical Measurements. Elemental analysis was carried out on a Perkin-Elmer 2400 II CHN analyzer. The inductively coupled plasma-atomic emission spectrometry (ICP-AES) analysis was performed by using a Shimadzu ICPE-9000 at the Research and Analytical Center for Giant Molecules (Tohoku Univ.). X-ray Fluorescence (XRF) spectra were recorded on a Rigaku NEX DE at the Rigaku corporation Tokyo plant. Solution and in the solid state (KBr pellets) absorption spectra (200-3300 nm) were recorded on a Hitachi U-4100 spectrophotometer at room temperature. Cyclic voltammetry (CV) and differential pulse voltammetry (DPV) measurements were recorded on a BAS model 650A electrochemical analyzer, using a glassy carbon (GC) working electrode and a platinum (Pt) auxiliary electrode under an atmosphere of N_2 at room temperature. The reference electrode consisted of a silver wire, inserted into a small glass tube fitted with a porous Vycor frit at the tip, filled with a MeCN solution containing 0.1 M $[n\text{Bu}_4\text{N}]ClO_4$ and 0.01 M $AgNO_3$. All three electrodes were immersed in 2 mL of a MeCN solution containing 0.1 M $[n\text{Bu}_4\text{N}]PF_6$ as the supporting electrolyte and 1 mM analyte. Redox potentials were measured relative to the Ag/Ag^+ redox couple. Spectroelectrochemical measurements were carried out in 0.1 M $[n\text{Bu}_4\text{N}]PF_6$ solution using Pt, Pt mesh, and the reference electrodes under an atmosphere of N_2. The magnetic measurement was performed using a magnetic property measurement system (MPMS-XL, Quantum Design) in the direct current mode. The sample was filled into a gelatin capsule (Matsuya) which was fixed in a plastic straw.

Collection of crystallographic data and structure refinements. A suitable single crystal of **1**·*x*H_2O was selected and mounted onto a MicroMount (MiTeGen) in an XtaLAB Synergy R, DW system, HyPix diffractometer. The crystal was kept at 120 K using a N_2 flow-type temperature controller during data collection. Using Olex2,[S1] the structure was solved with the ShelXT[S2] structure solution program using intrinsic phasing and refined with the ShelXL[S3] refinement package using least-squares minimization. A summary of the crystallographic data for **1**·*x*H_2O is shown in Table S1. The X-ray crystallographic coordinates used for the structure determination reported in this article have been deposited at the Cambridge Crystallographic Data Centre (CCDC) under deposition numbers CCDC-2104264. The data can be obtained free of charge from The Cambridge Crystallographic Data Centre via www.ccdc.cam.ac.uk/data_request/cif.

Simulations of magnetism. $\chi_m T$ was simulated using the program PHI with the spin Hamiltonian of equations S1 and S2:[S4]

$$\widehat{\mathcal{H}}_{ZEE} = \mu_B \widehat{\boldsymbol{S}} \cdot g \cdot \widehat{\boldsymbol{B}} \qquad \text{(eq. S1)}$$

$$\widehat{\mathcal{H}}_{SO} = \lambda \widehat{\boldsymbol{L}} \cdot \widehat{\boldsymbol{S}} \qquad \text{(eq. S2)}$$

where μ_B, g, λ, $\boldsymbol{S}$ and $\boldsymbol{L}$ with hats, and $\boldsymbol{B}$ refer to the Bohr magneton, g-factor, spin–orbit coupling constant, operators of spin and orbit, and magnetic field, respectively.

Table S1. Crystallographic data for **1**·xH$_2$O

Formula	$K_{0.2}Co_{2.4}Cr_2C_{36}O_{25.5}S_6H_{24}$
Formula weight	1310.16
Crystal size (mm^3)	0.2 × 0.2 × 0.1
Crystal system	triclinic
Space group	*P*-1 (No. 2)
a (Å)	12.6211(2)
b (Å)	14.7753(3)
c (Å)	16.6912(3)
α (°)	70.242(2)
β (°)	73.531(2)
γ (°)	88.9980(10)
V (Å^3)	2798.56(10)
T (K)	120
Z	2
D_{calc} (g cm^{-3})	1.555
F (000)	1303.0
μ(Mo Kα) (cm^{-1})	10.513
Reflections collected	89620
Independent reflections	17209
Data/restraints/parameters	17209/0/706
GOF on F^2	1.058
R_{int}	0.0518
R_1[a]	0.0620
wR_2[b] (all data)	0.1817

[a] $R_1 = \Sigma||F_o| - |F_c||/\Sigma|F_o|$. [b] $wR_2 = \{[\Sigma w(F_o^2 - F_c^2)^2]/[\Sigma w(F_o^2)^2]\}^{1/2}$.

Table S2. Selected bond distances of **1**·xH$_2$O

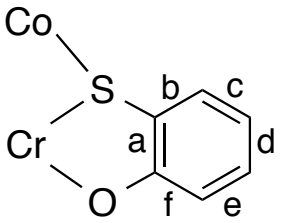

Bond distance [Å]	L1	L2	L3	L4	L5	L6
Co–S	2.3096(7)	2.2940(7)	2.3098(8)	2.2968(7)	2.3116(7)	2.3111(7)
Cr–S	2.3528(9)	2.3413(9)	2.3345(8)	2.3443(9)	2.3601(9)	2.3323(8)
Cr–O	1.979(2)	1.963(2)	1.969(2)	1.965(2)	1.974(2)	1.973(2)
C–S	1.775(3)	1.773(3)	1.766(3)	1.772(3)	1.777(3)	1.762(3)
C–O	1.349(3)	1.352(4)	1.351(4)	1.353(4)	1.354(4)	1.350(4)
C–C (a)	1.411(4)	1.404(4)	1.410(4)	1.407(4)	1.406(4)	1.414(4)
C–C (b)	1.402(5)	1.405(4)	1.401(4)	1.396(4)	1.403(5)	1.404(5)
C–C (c)	1.390(5)	1.383(5)	1.394(5)	1.386(5)	1.390(5)	1.384(6)
C–C (d)	1.395(6)	1.394(6)	1.387(6)	1.385(5)	1.390(5)	1.382(6)
C–C (e)	1.385(5)	1.384(5)	1.387(5)	1.386(4)	1.388(5)	1.393(5)
C–C (f)	1.396(4)	1.396(4)	1.398(4)	1.395(4)	1.399(4)	1.395(4)

Ligands 1–6 (L1–L6) contain S1, S2, S3, S4, S5, and S6, respectively. See also Figure 2.

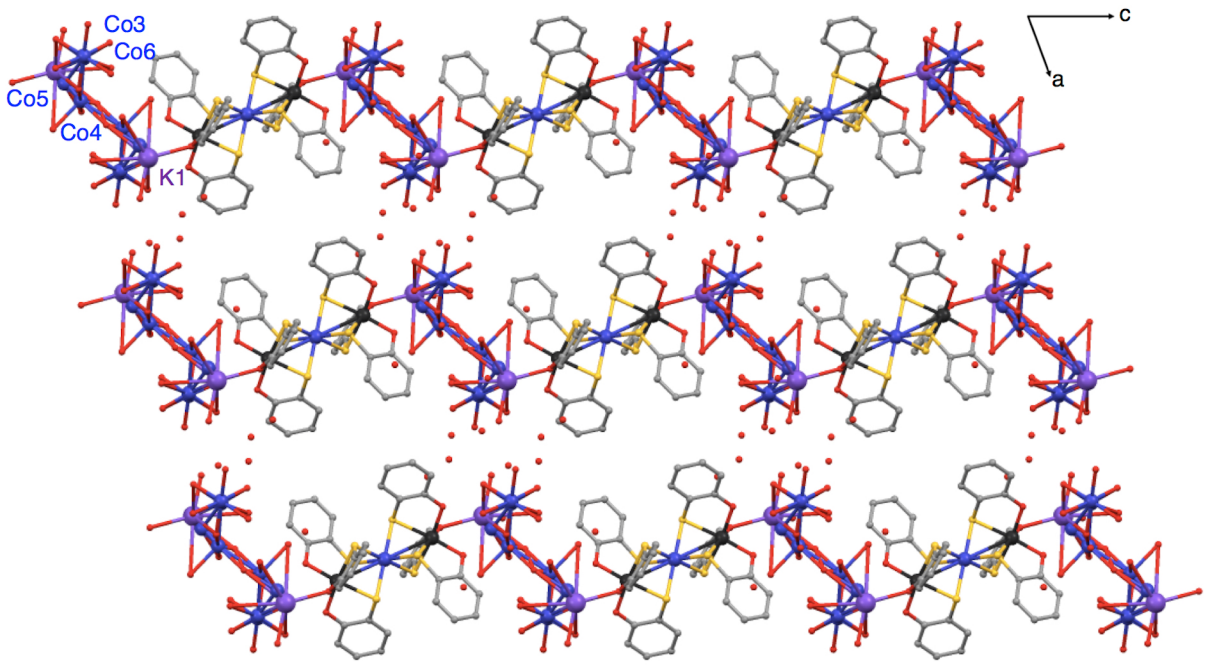

Figure S1. Crystal structure of **1**·xH$_2$O with a ball-and stick model. Color code: Cr = black, Co = blue, S = yellow, O = red, and C = grey. Hydrogen atoms have been omitted for clarity, and only selected atoms are labeled.

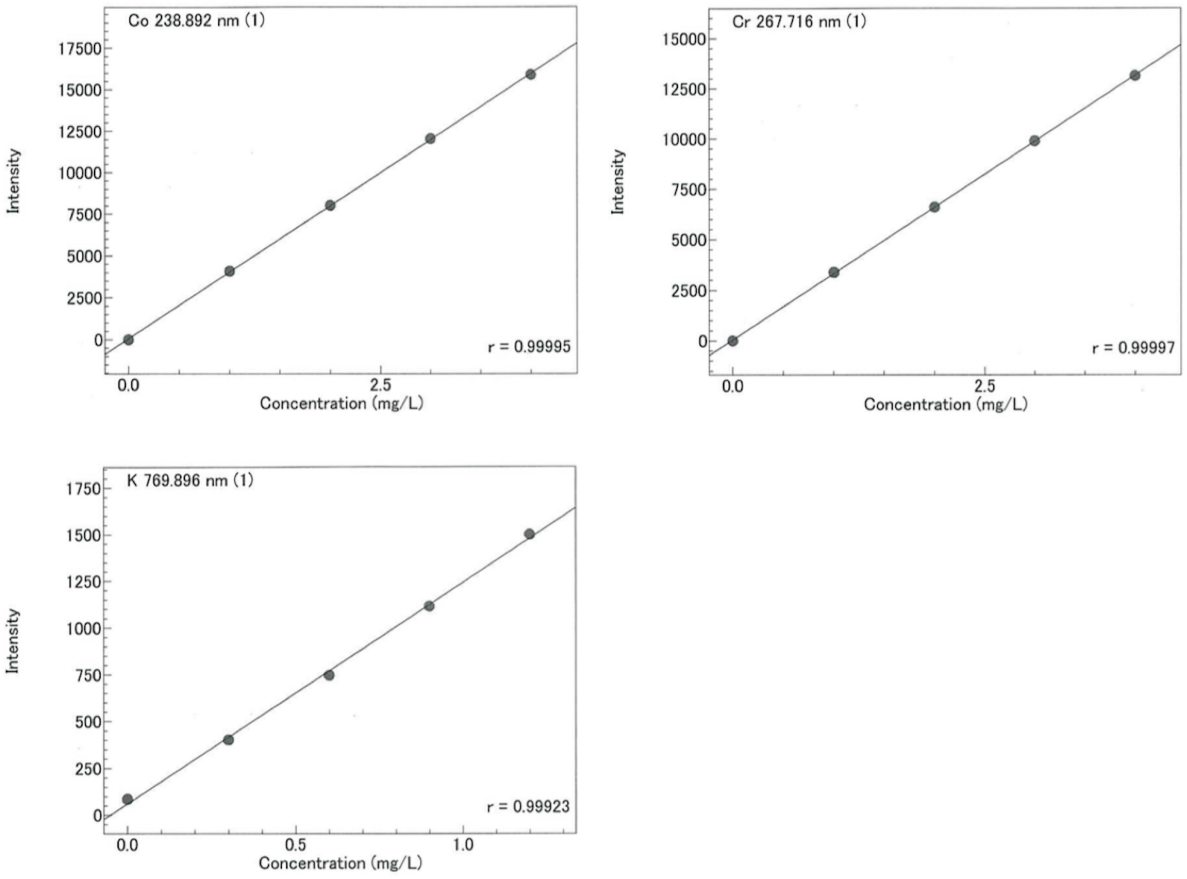

Figure S2. The calibration curve of ICP-AES analysis for Co, Cr, and K. Standards were used acidic (0.5% HNO_3 and 0.7% HCl) aqueous solutions containing Co:Cr:K=1:1:0.3, 2:2:0.6, 3:3:0.9, and 4:4:1.2 (ppm).

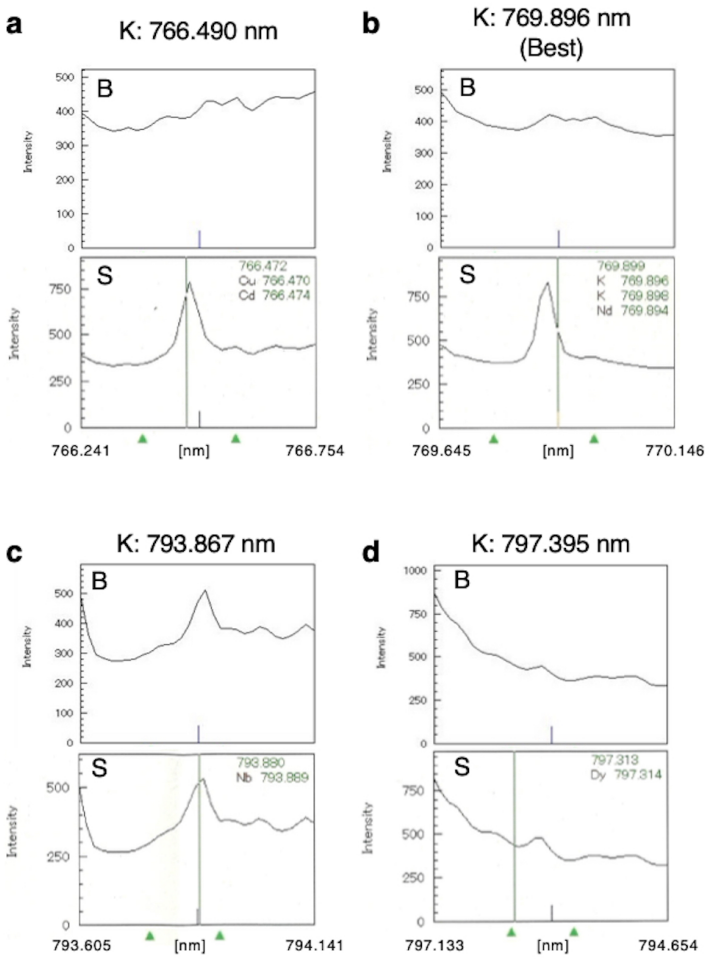

Figure S3. ICP-AES spectra of **1**·xH$_2$O (S: sample) in the range of K ion around (a) 766 nm, (b) 769 nm, (c) 793 nm, and (d) 797 nm, together with the blank solution (B). Inset elements are potential spectral interference species.

Table S3. Summary of ICP-AES measurement of **1**·xH$_2$O

Element	Co	Cr	K
[ppm]	2.63	2.00	0.163
[wt%]	12.4	9.4	0.77
[μM]	45	38	4.2
mol eq.	1.2	1.0	0.1

The sample solution was prepared form **1**·xH$_2$O (2.12 mg) and 100 mL acidic (0.5% HNO_3 and 0.7% HCl) deionized water.

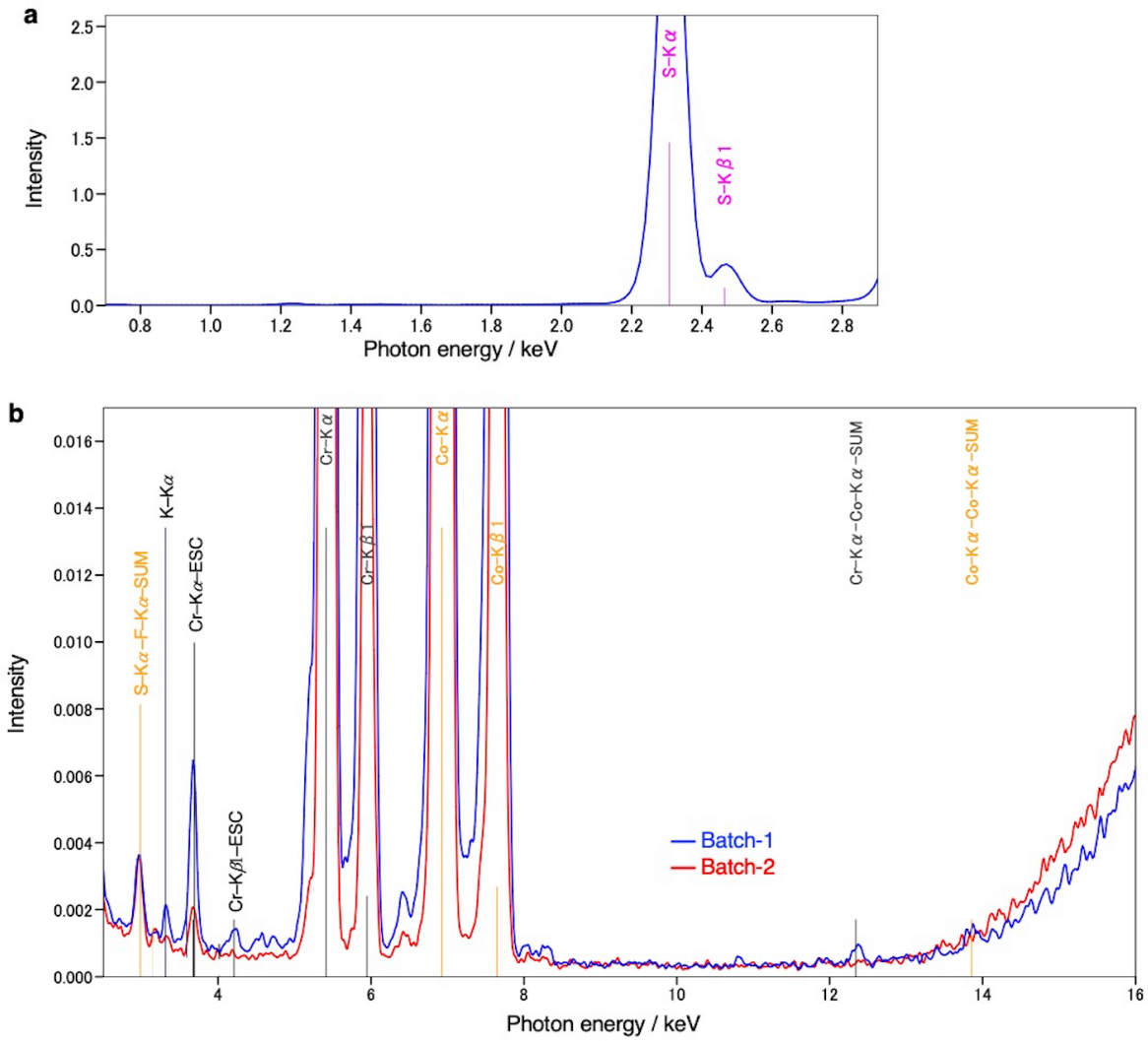

Figure S4. XRF spectra of **1**·xH$_2$O in the (a) low and (b) middle energy regions. *F is derived from a film or a sample container.

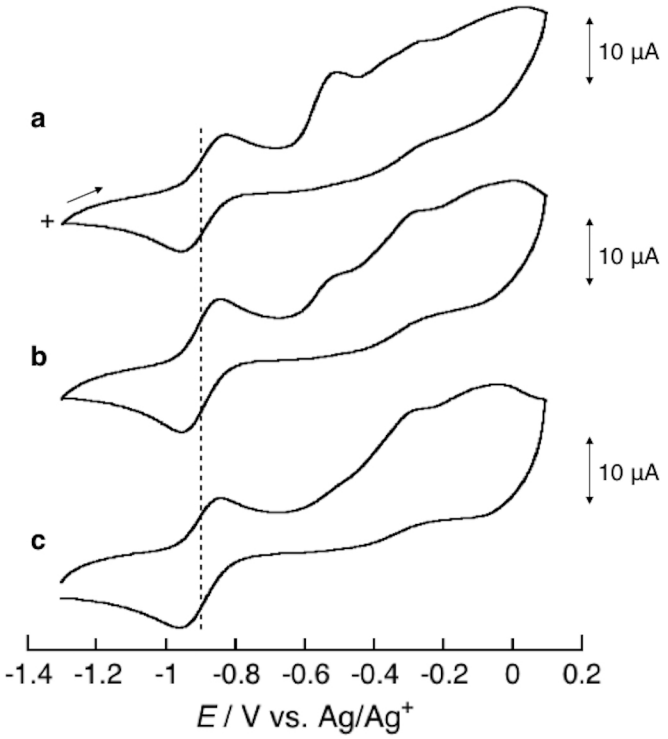

Figure S5. CVs of $[Me_4N]_3[fac\text{-}Cr(mp)_3]$ (1.0 mM) upon addition of (a) 0.5, (b) 0.75, and (c) 1.0 eq. of $Co^{II}(ClO_4)_2 \cdot 6H_2O$, measured at 50 mV s^{-1} with 0.1 M $[nBu_4N]PF_6$ in MeCN under an atmosphere of N_2 using GC, Pt, Ag/Ag^+ electrodes.

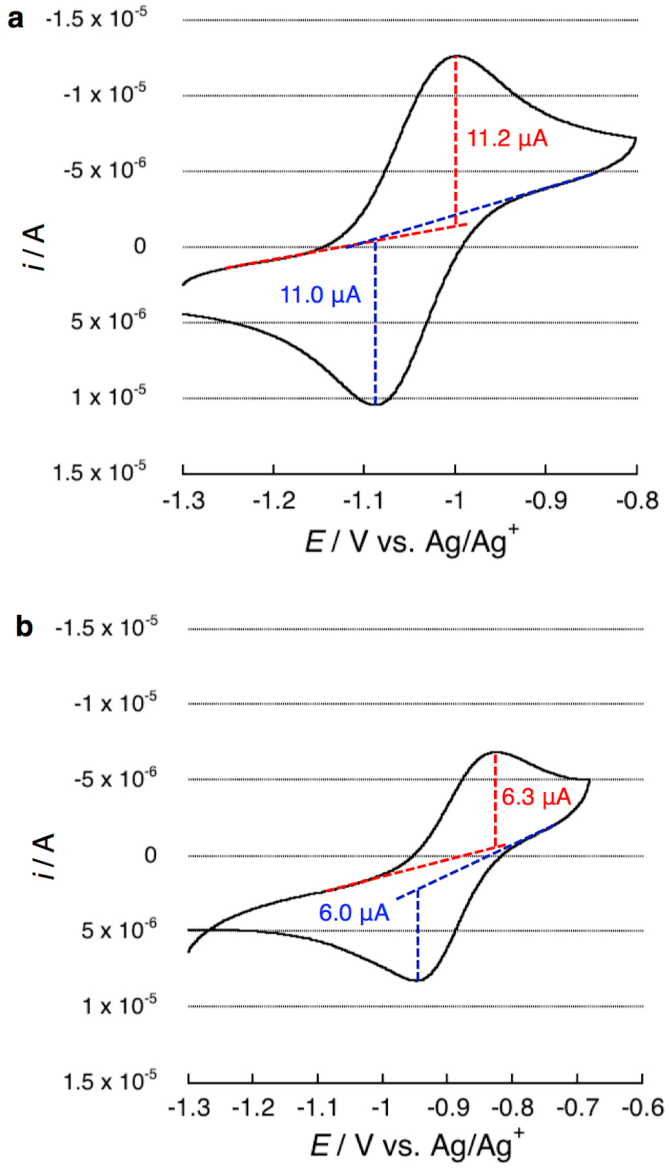

Figure S6. CVs of $[Me_4N]_3$[*fac*-$Cr(mp)_3$] (1 mM) upon addition of (a) 0 and (b) 0.5 eq. of $Co^{II}(ClO_4)_2 \cdot 6H_2O$, at the potential range around the first oxidation process measured at 50 mV s^{-1} with 0.1 M $[nBu_4N]PF_6$ in MeCN under an atmosphere of N_2 using GC, Pt, Ag/Ag^+ electrodes.

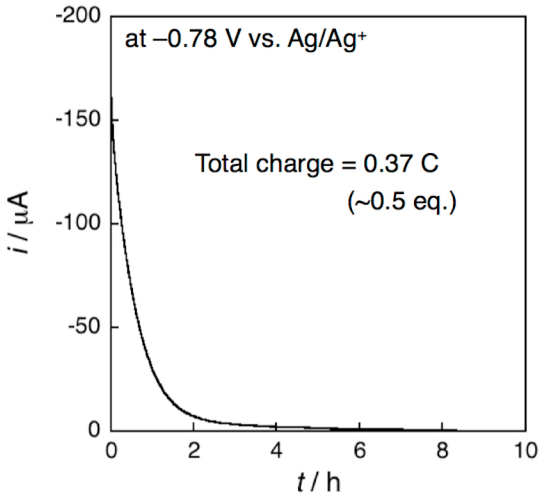

Figure S7. The *i*-*t* curve of $[Me_4N]_3[fac\text{-}Cr(mp)_3]$ (8.0 μmol) upon addition of 0.5 eq. of $Co^{II}(ClO_4)_2 \cdot 6H_2O$ (4.0 μmol), with 0.1 M $[nBu_4N]PF_6$ in MeCN under an atmosphere of N_2 using Pt and Ag/Ag^+ electrode. The counter Pt electrode was separated by porous glass.

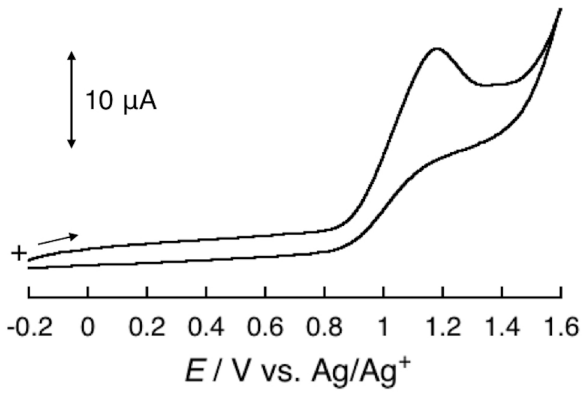

Figure S8. CV of $Co^{II}(ClO_4)_2 \cdot 6H_2O$ (1 mM) measured at 50 mV s^{-1} with 0.1 M $[nBu_4N]PF_6$ in MeCN under an atmosphere of N_2 using GC, Pt, Ag/Ag^+ electrodes.

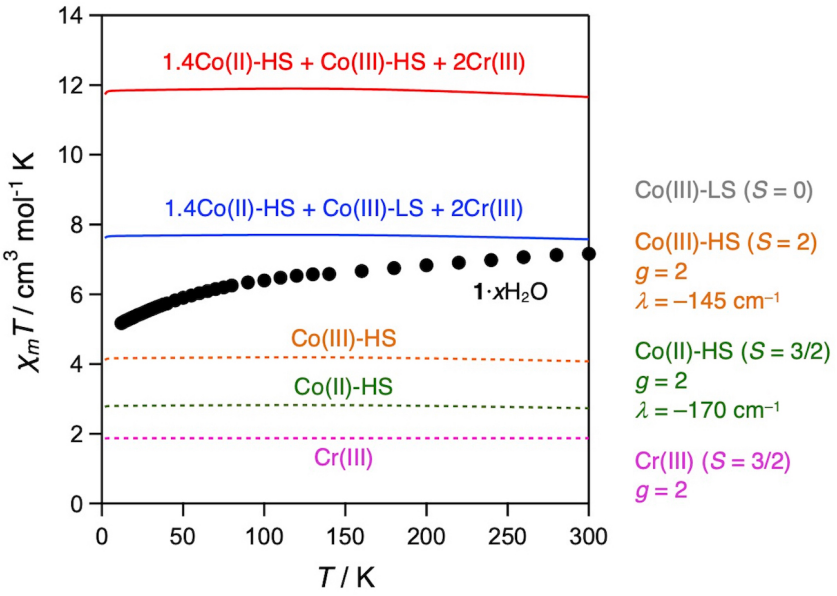

Figure S9. $\chi_m T$–T plots for **1**·xH$_2$O together with those of simulations and parameters (g-factor and spin-orbit coupling energy (λ)). HS and LS represent high-spin and low spin states, respectively.

References

(S1) O. V. Dolomanov, L. J. Bourhis, R. J. Gildea, J. A. K. Howard, H. Puschmann, *J. Appl. Crystallogr*. 2009, **42**, 339–341.

(S2) G. M. Sheldrick, *Acta Crystallogr., Sect. A: Found. Adv*. 2015, **A71**, 3–8.

(S3) G. M. Sheldrick, *Acta Crystallogr., Sect. C: Struct. Chem*. 2015, **C71**, 3–8.

(S4) N. F. Chilton, R. P. Anderson, L. D. Turner, A. Soncini, K. S. Murray, *J. Comput. Chem*. 2013, **34**, 1164–1175.